



Published in final edited form as:

*J Neurointerv Surg.* ; 16(8): 846–851. doi:10.1136/jnis-2023-020668.

## Report from the Society of Magnetic Resonance Angiography: Clinical applications of 7T Neurovascular MR in the assessment of intracranial vascular disease

Binbin Sui, MD<sup>1</sup>, Bhagya Sannananja, MD<sup>2</sup>, Chengcheng Zhu, PhD<sup>3</sup>, Niranjan Balu, PhD<sup>3,4</sup>,  
Laura Eisenmenger, MD<sup>5</sup>, Hediye Baradaran, MD<sup>6</sup>, Myriam Edjlali, MD<sup>7</sup>, Javier Romero,  
MD<sup>8</sup>, Prabhakar Rajiah, MBBS<sup>9</sup>, Rui Li, PhD<sup>10</sup>, Mahmud Mossa-Basha, MD<sup>3,4</sup>

<sup>1</sup>Tiantan Neuroimaging Center of Excellence, China National Clinical Research Center for Neurological Diseases, Beijing, China.

<sup>2</sup>Department of Radiology and Imaging Sciences, Emory University School of Medicine, Atlanta, GA, USA.

<sup>3</sup>Department of Radiology, University of Washington School of Medicine, Seattle, WA, USA.

<sup>4</sup>Vascular Imaging Lab, University of Washington, Seattle, WA, USA

<sup>5</sup>Department of Radiology and Medical Physics, University of Wisconsin School of Medicine and Public Health, Madison, WI, USA.

<sup>6</sup>Department of Radiology and Imaging Sciences, University of Utah School of Medicine, Salt Lake City, UT, USA

<sup>7</sup>Department of Radiology, APHP, Hôpitaux Raymond-Poincaré & Ambroise Paré, DMU Smart Imaging, GH Université Paris-Saclay, Paris, France.

<sup>8</sup>Radiology Department, Massachusetts General Hospital, Harvard Medical School, Boston, MA, USA.

<sup>9</sup>Department of Radiology, Mayo Clinic, Rochester, MN, USA.

<sup>10</sup>Center for Biomedical Imaging Research, Medical School, Tsinghua University, Beijing, China.

### Abstract

In recent years, ultra-high field MRI applications have been rapidly increasing in both clinical research and practice. 7T MRI allows improved depiction of smaller structures with high signal-to-noise ratio, and, therefore, may improve lesion visualization, diagnostic capabilities, and thus potentially affect treatment decision-making. Incremental evidence emerging from

---

Corresponding authors: Mahmud Mossa-Basha, MD, 1959 NE Pacific St, Seattle, WA 98195, mmossab@uw.edu, Twitter: @mossabas, Phone: 206-598-3845; Binbin Sui, MD, No. 119 South Fourth Ring West Road, Fengtai District, Beijing 100070, China, reneesui@163.com.

**Author contribution:** All authors contributed substantially to the conception and design of the work, drafting and revising of the manuscript, final approval of the manuscript, and agreeable to be accountable for all aspects of the work.

**Ethics Approval Disclosure Statement:** Institutional Review Board approval was not necessary for the contributing institutions for this review article. The article did not include any research investigation or data and all imaging examples are de-identified.

**Conflicts of interest:** The authors have none.

research over the past two decades has provided a promising prospect of 7T MRA in the evaluation of intracranial vasculature. The ultrahigh resolution and excellent image quality of 7T MRA allow us to explore detailed morphological and hemodynamic information, detect subtle pathological changes in early stages, and provide new insights allowing for deeper understanding of pathological mechanisms of various cerebrovascular diseases. However, along with the benefits of ultrahigh field strength, some challenges and concerns exist. Despite these, ongoing technical developments and clinical-oriented research will facilitate the widespread clinical application of 7T MRA in the near future. In this review article, we summarize technical aspects, clinical applications, and recent advances of 7T MRA in the evaluation of intracranial vascular disease. The aim of this review is to provide a clinical perspective for the potential application of 7T MRA for the assessment of intracranial vascular disease, and to explore possible future research directions implementing this technique.

---

## Introduction

Since regulatory approval in 2017, commercial 7T MRI systems have been installed for clinical use in multiple academic institutions, with resultant developmental acceleration. The primary clinical advantages of 7T MRI systems include higher signal-to-noise ratio, contrast-to-noise ratio, spatial resolution, and stronger susceptibility contrast that can improve lesion detection, conspicuity, and characterization compared to 1.5T and 3T MRI field strengths. Intracranial neurovascular MR techniques have significant incremental benefits when performed using a 7T magnet. Although neurovascular MR techniques at 1.5T and 3T are well established in the evaluation of neurovascular diseases including intracranial stenosis, aneurysms, and arteriovenous malformations, they are limited in the evaluation of cerebral small vessel disease (CSVD), primarily due to spatial resolution constraints. Some very promising applications of 7T imaging includes MRA and its improved visualization of lenticulostriate branches, potentially providing better elucidation of CSVD pathophysiology, and improve detection of small cerebral aneurysms and differentiate pathology from normal arterial variants. 7T vessel wall MR (VWI) can improve depiction of arterial wall lesions, and potentially better characterize lesions and identify vulnerable features. There are 35 7T MRI systems installed in North America, including 16 clinical units. The scanners cost at baseline nine million dollars, with enhancements potentially increasing costs by millions, and the additional millions in construction costs required for room design, specifications, and unit installation.

The Society of Magnetic Resonance Angiography, a society comprised of vascular and neurovascular MR experts, wrote this article in order to help better educate neurointerventionalists and other neuroscience clinicians on the clinical value of 7T neurovascular imaging and how it may potentially improve vascular disease diagnosis. We review the technical advantages and limitations of 7T neurovascular MR, followed by a detailed discussion of the utility and applications of 7T neurovascular MR in the assessment of intracranial vascular diseases.

## Advantages and technical challenges of 7T compared to lower field strengths

With 7T TOF-MRA, there is a three-fold increase of SNR and four-fold increase in contrast-to-noise (CNR) compared to 3T<sup>1</sup>. This allows higher resolution imaging than 3T (Supplemental Table 1 reviews the advantages and disadvantages of 7T over 3T MR). With the ability to achieve 0.2-0.3 mm isotropic resolution, 7T improves depiction of small arteries and increased conspicuity of pathology. Ultra-high magnetic fields also generate prolonged blood T1 relaxation times, enhanced in-flow and phase-contrast effect, and better vascular conspicuity and CSF suppression, which can enhance MRA image quality. Furthermore, higher field strengths offer strong contrast enhancement that may increase sensitivity in detecting intracranial vessel wall inflammatory lesions.

7T vessel wall MR (VWI) also provides improved vascular conspicuity and CSF suppression than 3T. Even at similar resolutions (~0.5mm<sup>3</sup>), 7T VWI could detect more arterial wall lesions<sup>2</sup>. 7T VWI can demonstrate thin vessel walls, overcoming the insufficient resolution seen on 3T. 7T VWI is superior in displaying arterial anatomy, detecting small lesions, and identifying overall plaque burden relative to 3T VWI<sup>2</sup>.

7T MR can improve the spatiotemporal resolution of 4D-flow imaging, thus enhancing hemodynamic assessment. Time-resolved 7T 3D PC-MR shows smoother streamlines and more accurate velocity vectors of the Circle of Willis compared to 3T<sup>3</sup>. Acceleration techniques have also been employed to improve resolution (~0.5mm<sup>3</sup> isotropic) for 7T 4D-flow imaging in comparable scan times (10 mins) and can enable quantification of penetrating arteries.

7T susceptibility-weighted imaging (SWI) permits visualization and quantification of deep medullary veins. Dual-echo arteriovenography at 7T can improve visualization of small vessels on MRA and SWI-MRV due to the increased SNR and susceptibility contrast compared to 3T.

Despite these advantages, 7T MRA also faces several challenges, including larger magnetic field inhomogeneity, increased specific absorption rate (SAR), increased contraindications and safety concerns, and longer acquisition times (Supplemental Table 2). The spatially-varying transmit B<sub>1</sub> (B<sub>1+</sub>) inhomogeneity is a major concern for high-field MRI and has been found to generate suboptimal TOF contrast. After a B<sub>1+</sub> shimming system was implemented, excitation homogeneity could be improved by a factor of 2.2–2.6, resulting in better peripheral vessel visualization on TOF-MRA<sup>4</sup>. Another challenge is the increased local and global SAR at 7T, which limits the optimal setting of the sequences and can raise safety concerns. Pulse setting adjustments and the application of designed RF coils have been suggested as potential approaches to mitigate SAR-related issues<sup>5,6</sup>. Acceleration techniques, including compressed-sensing (CS) and generalized auto-calibrating partially parallel acquisition (GRAPPA)-based techniques have been implemented to improve scan time and patient compliance. CS acceleration with an acceleration factor of 7.2 achieved 0.31 mm isotropic resolution in 5 minute scan time<sup>7</sup> (Figure 1). However, to obtain high

quality images at even higher resolution ( $\sim 150 \mu\text{m}^3$ ), motion-correction to mitigate arterial pulsation artifacts may be necessary for small vessel delineation.

## Intracranial atherosclerotic plaque

While clinical 1.5T or 3T TOF-MRA are the first-line imaging tools for intracranial vasculature assessment, 7T MRA can depict intracranial vessels with better conspicuity. An early study showed the ability of 7T TOF-MRA to depict the entire length of first and second order Circle of Willis branches, with 88% lower percentage of visualization at 1.5T and 3T<sup>8</sup>. The accuracy of 7T MRA for stenosis measurement has proven to be highly accurate in phantom studies<sup>9</sup>. However, the comparison of stenosis measurement using 7T non-contrast TOF-MRA, contrast-enhanced MRA, and VWI relative to the gold standard DSA is still needed.

The enhanced spatial resolution with sufficient SNR of 7T VWI provides higher wall-lumen contrast and improved CSF signal suppression, improving image sharpness and quality relative to 3T<sup>2</sup>. 7T VWI enables more accurate artery wall thickness measurements compared to 3T with histology as the reference<sup>10</sup>, improving identification of subtle non-stenotic vessel wall lesions and providing more accurate plaque burden assessment. 7T VWI studies have demonstrated that intracranial plaque burden is associated with certain vascular risk factors, worse memory, and lower executive functioning<sup>11</sup>. In patients without a history of cerebrovascular disease,  $7.3 \pm 4.9$  lesions were discovered on VWI. The clinical significance of these small lesions is unclear, but considering their high prevalence, identification of subtle lesions could potentially help in determining stroke etiology in patients initially classified as cryptogenic stroke, help define optimal treatment, and may improve patient outcomes. In addition, early and sensitive identification of vascular lesions could help us better understand the continuum of vascular aging versus pathologic vascular disease, and the impact vascular disease can have on neurodegenerative conditions.

Ex-vivo 7T multi-parametric VWI imaging (0.1mm isotropic resolution) of intracranial atherosclerotic disease (ICAD) advanced plaque composition indicated a hypointense signal on PD-, T2-, and T2\*WI corresponded with foamy macrophages, increased proteoglycans, or lipid-rich core<sup>12</sup>. With the continuous improvement of in vivo 7T VWI resolution, plaque composition analysis in the intracranial arteries, may be possible in the near future.

Clinical studies have reported the features of culprit ICAD on 3T VWI, including a higher degree of contrast enhancement, positive remodeling, and intraplaque hemorrhage<sup>13</sup>. 7T may better delineate signal characteristics and plaque surface morphology (Supplemental Figure 1). ICAD enhancement features, suggested as a high-risk plaque characteristic, have been qualitatively comparable between 7T and 3T VWI, with higher contrast-ratio and concentric morphology in culprit than non-culprit plaques<sup>14</sup>. Though additional literature evidence utilizing 7T VWI for plaque composition analysis is still needed, with increased lesion depiction, improved morphological ICAD characterization, and developing automated quantitative methods, ICAD characterization has the potential to be a major area of clinical advancement in 7T VWI.

7T VWI wall enhancement characteristics post-thrombectomy have been assessed, with one study prospectively evaluating arterial wall enhancement in 49 ischemic stroke patients within 3 months of symptoms, 14 of which underwent intra-arterial thrombosuction and 35 who did not undergo intra-arterial therapy<sup>15</sup>. 79% of thrombosuction patients compared to 49% without intra-arterial therapy showed ipsilateral arterial wall enhancement. In the treatment group, enhancing lesions were more frequently seen on the ipsilateral side and were more often concentric relative to the contralateral side, while no differences were seen in the non-treatment group. These findings are similar to those seen on 3T VWI where there was increased presence of concentric enhancing lesions ipsilateral to mechanical thrombectomy, corresponding with increased number of passes and increased likelihood of hemorrhagic conversion<sup>16</sup>, with stent retriever devices associated with a higher likelihood and degree of enhancement compared to aspiration devices. These findings likely relate to arterial wall injury and resultant inflammation from device deployment.

### Perforator visualization and associations with disease

Increased resolution with 7T MR allows improved evaluation of lenticulostriate (LSAs)<sup>17</sup>, pontine perforator (PAs), and cortical arteries (Figure 1). A recent study achieved 140 $\mu$ m resolution on 7T TOF-MRA with visualization of pial arteries<sup>18</sup>. Improved conspicuity and visualization of LSAs can have a number of potential clinical benefits, including: 1) depiction of ostial involvement by ICAD for etiologic diagnosis of deep infarcts, 2) imaging biomarker for future longitudinal studies to determine the associations and causation of LSA pathology, CSVD, and cognitive impairment, 3) better detection and longitudinal evaluation of small artery inflammatory vasculopathies, and 4) better detection of small cerebral aneurysms.

Perforator evaluation on 7T MRA has been an intense area of recent investigation. There are fewer LSAs supplying the basal ganglia in stroke patients compared with age-matched controls on 7T MRA, and in patients with LSA territorial infarcts, occlusive changes in the LSAs on 7T VWI were frequent and were associated with increased craniocaudal infarct extension<sup>17</sup>. ICAD involving the middle cerebral artery (MCA) or basilar artery (BA) may partially or completely block perforator ostia, termed “branch atheromatous disease (BAD)”, leading to perforator territory infarcts. ICAD involving LSA origins on 7T-MRA and VWI was independently associated with perforator territory infarct (OR 28.51; 95% CI 6.34-181.02)<sup>19</sup> (Figure 2).

CSVD is a heterogenous entity characterized by chronic, progressive vasculopathy affecting the cerebral small arteries, arterioles, capillaries, and venules. CSVD is associated with ischemic strokes, vascular dementias, and plays a key role in the pathogenesis of Alzheimer’s dementia. Instead of relying on indirect parenchymal imaging markers for CSVD diagnosis, 7T MRA can assess structural features such as identification of the number of LSA stems and branches, average length and tortuosity, and recognition of any narrowing or interruptions, thus providing a new perspective for the understanding of CSVD pathogenesis. 7T TOF-MRA has found significant differences in LSA morphology between patients with hypertension or chronic stroke and healthy subjects. In subcortical vascular dementia, there is a significantly decreased number of LSA branches and stems in

patients with CSVD risk factors<sup>25</sup>. 7T VWI might be useful in elucidating the pathological features of small arteries in CSVD. Association between large artery ICAD with onset and progression of CSVD needs to be verified with further studies. A sub-analysis of the SMART-MR study (n=130) found patients with higher burden of ICAD also had more extensive CSVD<sup>26</sup>. Higher plaque burden corresponded with white matter hyperintensity severity, subcortical and deep gray matter infarcts, and vascular lacunes.

7T SWI depiction of venules provides an avenue to further evaluate venous findings in CSVD. Shaaban et al. reported 42% more tortuous anatomy of venules compared to straight anatomy in their CSVD and AD cohorts (n= 53, median, 1.42; 95% CI, 1.13–1.62)<sup>27</sup>.

## Non-atherosclerotic intracranial vasculopathies

Though the literature is sparse on 7T cerebrovascular imaging of non-atherosclerotic, non-aneurysmal intracranial arteriopathies, the few studies performed have promising results, showing 7T VWI can better depict wall lesions as compared to 3T VWI (Figure 3). In three cases of biopsy-proven giant cell arteritis, 7T VWI revealed strong enhancement of the superficial cranial arteries on contrast-enhanced T1-weighted images, with superior image quality to 3T MRI<sup>20</sup>. Additionally, 7T T1WI has been applied to systemic lupus erythematosus (SLE) to detect micro-cerebrovascular changes, presenting as minute punctate or linear hyperintense lesions in subcortical and/or cortical areas<sup>21</sup>. Currently, there are no reports on vasculitis using 7T MRA, but the improved resolution (up to ~150 $\mu$ m) could enable visualization of CNS vasculitis-related changes.

Excellent 7T MRA angioarchitecture depiction improves moyamoya disease (MMD) evaluation. In a case-control study including 12 MMD patients, 7T MRI/MRA found significantly more flow voids, representing collaterals, on T2-weighted imaging (3.71 vs. 1.17) and higher signal intensity of these collaterals on TOF-MRA (7.16 vs. 4.75) than 3T (both  $p < 0.001$ )<sup>22</sup>. Using 7T TOF-MRA with 0.22 $\times$ 0.22 $\times$ 0.41 mm<sup>3</sup> resolution, the deep-seated collaterals detected were equivalent to those represented on DSA; however, 7T MRA had the advantage of not suffering from overlapping vessels obscuring vascular anatomy<sup>23</sup>.

7T MRA has facilitated increased microbleed and microaneurysm detection (Figure 4). 7T SWI (0.5 $\times$ 0.5 $\times$ 0.75 mm resolution) and TOF-MRA (0.5 $\times$ 0.4 $\times$ 0.42 mm) fusion images improved detection of bleeding sources in hemorrhagic MMD. Microaneurysms arising from the peripheral collaterals, measuring between 0.56-0.96 mm in diameter, were discovered in 4 out of 10 cases by 7T TOF-MRA<sup>24</sup>. Microstructural pathology detection requiring submillimeter-resolution imaging could be a possible clinical application of 7T MRA.

## Hemodynamic imaging

Quantitative flow assessment based on PC-MRI can be valuable for pathophysiological hemodynamic status assessment in patients with cerebrovascular disease, with 7T hemodynamic imaging enabling smaller vascular structure assessment. Previous 3T 4D-flow data showed proximal intracranial artery hemodynamic alterations are associated with cognitive performance, brain atrophy, and Alzheimer's A $\beta$ -42 profile<sup>28</sup>. Evaluation and characterization of small arteries and their contribution to dementia, however, is limited



on 3T owing to limited achievable spatial resolution. Using cardiac-gated 2D PC-MRI, 7T MRI can directly measure velocities in cerebral microvessels with a diameter  $>80\ \mu\text{m}$ . A 3T and 7T comparison study showed that perforator velocity and pulsatility measurements are field-strength dependent<sup>29</sup>.

Aging and vascular risk factors increase large artery stiffness, which in turn results in increased arterial pulsatility of distal small arteries, leading to microcirculatory damage. Pulsatility index (PI) is calculated by Gosling's equation [ $\text{PI} = (\text{peak systolic velocity} - \text{peak diastolic velocity}) / \text{mean velocity}$ ]. Increased arterial pulsatility is associated with microstructural brain damage and small vessel injury, indicating a potential mechanistic link between aortic stiffening, brain lesions and cognitive impairment. PI in patients with lacunar infarcts and deep intracranial hemorrhage was higher than in controls, while no velocity differences were detected<sup>30</sup>, suggesting pulsatility increases before the absolute velocity change.

The perforating arteries of the centrum semiovale and basal ganglia have been the focus of CSVD hemodynamic studies. In healthy controls, LSA PI significantly increased and damping factor significantly decreased with age<sup>31</sup>. 7T 4D-flow MRI can provide velocity measurements in the microcirculation, potentially capturing pre-clinical pathologic changes before irreversible structural damage occurs in CSVD or other cerebrovascular diseases. Increased pulsatility from wall stiffening is also likely a manifestation of vascular wall disease itself.

There are a number of potential challenges and limitations to 7T 4D-flow MRI. One challenge is partial volume effects due to limited voxel inclusion may distort the measurements. Velocity of perforating arteries may be underestimated while pulsatility may be overestimated by simulations. Parameter optimization and velocity corrections can yield superior hemodynamic estimates in suitable acquisition times. Ghosting artifacts arising from subject movement or pulsating large arteries also require manual or automated censoring to prevent obscuration of the targeted microvessels. Overcoming these 7T MRA challenges may further enhance the performance of 7T MRA in clinical applications.

## Intracranial aneurysms

MRA is widely used for intracranial aneurysm detection, evaluation, and follow-up, however, the sensitivity of 1.5T and 3T MRA for small aneurysm ( $<5\text{mm}$ ) detection is limited, and the differentiation between small aneurysms and infundibula can be challenging. The image quality of 7T TOF-MRA and VWI is better than 1.5T or 3T in displaying aneurysm structure and morphology<sup>8</sup>. Compared with the gold standard DSA, 7T TOF-MRA demonstrated excellent delineation of unruptured aneurysms (UIAs) with diameters between 0.9-36 mm and added diagnostic value in differentiating aneurysms from anatomic variants including infundibula or perforators<sup>32</sup>. In a study with 30 patients, the diagnosis of suspected intracranial aneurysm determined on 3T was changed to vascular variant in 66% of cases<sup>32</sup>.

Aneurysm wall enhancement is associated with aneurysm symptoms, subsequent aneurysmal growth, rupture risk, and aneurysm recurrence post-intervention<sup>8</sup>. Improved image quality at 7T allows quantification of aneurysm wall thickness and enhancement. 7T microstructure evaluation facilitated discovery that inner wall enhancement was correlated with neovascularization with adjacent thrombus, while outer wall enhancement was associated with vasa vasorum ingrowth<sup>8</sup>. Samaniego et al found an association between parent artery wall enhancement in proximity to the neck of UIAs and circumferential aneurysm wall enhancement, suggesting that parent artery inflammation may correlate with aneurysm formation and instability<sup>33</sup>.

Hemodynamic assessment can be beneficial for the evaluation of UIA rupture risk. 7T may provide more detailed anatomic assessment than 3T, improving the accuracy of computational fluid dynamic (CFD) simulation modeling. There is an inverse correlation between wall shear stress (WSS) and local aneurysm wall thickness and wall enhancement<sup>8</sup>. The pattern of enhancement and WSS can be mapped regionally, demonstrating the aneurysm neck having high WSS and lower likelihood of enhancement, while the dome and body had low WSS and higher likelihood of enhancement. 7T may also offer new acceleration algorithms, facilitating faster 4D-flow sequences that may be clinically feasible<sup>34</sup>. 4D-flow imaging studies and the CFD simulations based on 7T MRA may provide more key insights into the pathophysiological processes leading to aneurysm growth and rupture, and could become valuable tools in diagnostic armamentariums.

## Vascular Malformations

MRI plays an important role as a non-invasive technique in lesion assessment, stereotactic radiosurgery planning and follow-up imaging of vascular malformations. Due to its superior spatial resolution, 7T-MRA depicts the nidus, supply arteries and draining veins of intracerebral AVMs accurately, with image quality comparable to DSA<sup>35</sup>. However, venous saturation for AVMs at 7T-TOF-MRA is inferior relative to 3T-MRA, even when using optimized venous saturation pulses<sup>36</sup>. On the other hand, 7T time-resolved MRA shows outstanding delineation of AVM features and enables clear visualization of draining veins otherwise not depicted on 3T MRA<sup>37</sup>. With increased penetration of 7T MRI scanners, and increased utilization of 7T-MRA for assessment of AVM, this could potentially reduce the reliance on DSA for AVM follow-up or evaluation of equivocal cases.

7T T2\*GRE and SWI, due to increased susceptibility artifacts, will show increased number and conspicuity of slow-flow vascular malformations, including cerebral cavernous malformations (CCMs). In addition, cerebral venous variant anatomy on 7T high-resolution (0.25 mm<sup>2</sup> in-plane) SWI correlated with sporadic or familial CCMs<sup>38</sup>. Sporadic CCMs were associated with local venous abnormalities involving larger outflow vessels, whereas familial CCMs often exhibited normal venous anatomy. Severe artifacts near the skull base, however, should be considered as a limitation of 7T SWI and T2\*GRE, limiting lesion detection; differences in lesion size were also observed between 1.5T and 7T T2\* GRE, with discrepancies of up to 11%, which should be considered during interpretation<sup>39</sup>.



There are a number of immediate use applications for 7T Neurovascular MR, and potential future application (Supplemental Table 3), however, there are multiple questions that need to be addressed with future 7T MRA studies. Considering the current challenges of 7T MRA, development and employment of acceleration techniques, efficient RF coils, and novel sequences are essential for acquisition of high-quality whole brain coverage datasets in acceptable scan times without exceeding SAR (heating) limits. Verification of the reproducibility and reliability of 4D-flow imaging in intracranial vascular diseases is also necessary. Investigations on the early pathological changes of perforators and small cortical vessels, as well as the characteristic changes during the progression of vascular lesions, would be necessary for the establishment of the diagnostic criteria for intracranial large artery and small vessel diseases. So far, 7T MRA studies have reported interesting findings and insightful observations in case series. Longitudinal 7T MRA studies on various cerebrovascular diseases with larger sample sizes may provide better evidence for promotion of 7T MRA applications in clinical practice, including stronger evidence supporting changes to clinical management with the use of 7T imaging.

## Conclusion

7T MRA is promising for the assessment of intracranial vascular diseases. With ultrahigh resolution and SNR, 7T MRA can identify subtle lesions not otherwise detected on 3T, potentially providing additional value in cryptogenic cerebrovascular disease. In addition, its unique ability to assess small vessels and their hemodynamic characteristics can provide pathophysiological insights and new biomarkers for small vessel diseases.

## Supplementary Material

Refer to Web version on PubMed Central for supplementary material.

## Funding:

The project was supported with funding from NIH R01NS125635.

## References

1. Pohmann R, Speck O, Scheffler K. Signal-to-noise ratio and MR tissue parameters in human brain imaging at 3, 7, and 9.4 tesla using current receive coil arrays. *Magn Reson Med*. 2016;75(2):801–809. [PubMed: 25820458]
2. Hartevelde AA, van der Kolk AG, van der Worp HB, et al. High-resolution intracranial vessel wall MRI in an elderly asymptomatic population: comparison of 3T and 7T. *Eur Radiol*. 2017;27(4):1585–1595. [PubMed: 27387876]
3. van Ooij P, Zwanenburg JJM, Visser F, et al. Quantification and visualization of flow in the Circle of Willis: time-resolved three-dimensional phase contrast MRI at 7 T compared with 3 T. *Magn Reson Med*. 2013;69(3):868–876. [PubMed: 22618854]
4. Schmitter S, Wu X, Adriany G, Auerbach EJ, Urbil K, Moortele P-F. Cerebral TOF angiography at 7T: Impact of B1 (+) shimming with a 16-channel transceiver array. *Magn Reson Med*. 2014;71(3):966–977. [PubMed: 23640915]
5. Guérin B, Gebhardt M, Cauley S, Adalsteinsson E, Wald LL. Local specific absorption rate (SAR), global SAR, transmitter power, and excitation accuracy trade-offs in low flip-angle parallel transmit pulse design. *Magn Reson Med*. 2014;71(4):1446–1457. [PubMed: 23776100]

6. Seo J-H, Han Y, Chung J-Y. A Comparative Study of Birdcage RF Coil Configurations for Ultra-High Field Magnetic Resonance Imaging. *Sensors (Basel)*. 2022;22(5).
7. Meixner CR, Liebig P, Speier P, et al. High resolution time-of-flight MR-angiography at 7 T exploiting VERSE saturation, compressed sensing and segmentation. *Magn Reson Imaging*. 2019;63:193–204. [PubMed: 31434005]
8. Diab R, Chang D, Zhu C, et al. Advanced cross-sectional imaging of cerebral aneurysms. *Br J Radiol*. 2023;96(1141):20220686. [PubMed: 36400095]
9. Herz S, Stefanescu MR, Lohr D, et al. Effects of image homogeneity on stenosis visualization at 7 T in a coronary artery phantom study: With and without B1-shimming and parallel transmission. *PLoS One*. 2022;17(6):e0270689. [PubMed: 35767553]
10. Hartevelde AA, Denswil NP, Van Hecke W, et al. Ex vivo vessel wall thickness measurements of the human circle of Willis using 7T MRI. *Atherosclerosis*. 2018;273:106–114. [PubMed: 29715587]
11. Zwartbol MHT, van der Kolk AG, Ghaznawi R, et al. Intracranial atherosclerosis on 7T MRI and cognitive functioning: The SMART-MR study. *Neurology*. 2020;95(10):e1351–e1361. [PubMed: 32631923]
12. van der Kolk AG, Zwanenburg JJ, Denswil NP, et al. Imaging the intracranial atherosclerotic vessel wall using 7T MRI: initial comparison with histopathology. *AJNR American journal of neuroradiology*. 2015;36(4):694–701. [PubMed: 25477359]
13. Wang Y, Liu X, Wu X, Degnan AJ, Malhotra A, Zhu C. Culprit intracranial plaque without substantial stenosis in acute ischemic stroke on vessel wall MRI: A systematic review. *Atherosclerosis*. 2019;287:112–121. [PubMed: 31254918]
14. Fakhri R, Roa JA, Bathla G, et al. Detection and Quantification of Symptomatic Atherosclerotic Plaques With High-Resolution Imaging in Cryptogenic Stroke. *Stroke*. 2020;51(12):3623–3631. [PubMed: 32998652]
15. Lindenholz A, van der Schaaf IC, van der Kolk AG, et al. MRI Vessel Wall Imaging after Intra-Arterial Treatment for Acute Ischemic Stroke. *AJNR American journal of neuroradiology*. 2020;41(4):624–631. [PubMed: 32139427]
16. Seo WK, Oh K, Suh SI, Seol HY. Clinical Significance of Wall Changes After Recanalization Therapy in Acute Stroke: High-Resolution Vessel Wall Imaging. *Stroke*. 2017;48(4):1077–1080. [PubMed: 28258254]
17. Miyazawa H, Natori T, Kameda H, et al. Detecting lenticulostriate artery lesions in patients with acute ischemic stroke using high-resolution MRA at 7 T. *Int J Stroke*. 2019;14(3):290–297. [PubMed: 30299228]
18. Bollmann S, Mattern H, Bernier M, et al. Imaging of the pial arterial vasculature of the human brain in vivo using high-resolution 7T time-of-flight angiography. *eLife*. 2022;11.
19. Bai X, Fan P, Li Z, et al. Evaluating Middle Cerebral Artery Plaque Characteristics and Lenticulostriate Artery Morphology Associated With Subcortical Infarctions at 7T MRI. *J Magn Reson Imaging*. 2023.
20. Goll C, Thormann M, Hofmüller W, et al. Feasibility study: 7 T MRI in giant cell arteritis. *Graefes archive for clinical and experimental ophthalmology = Albrecht von Graefes Archiv fur klinische und experimentelle Ophthalmologie*. 2016;254(6):1111–1116.
21. Murata O, Sasaki N, Sasaki M, et al. Detection of cerebral microvascular lesions using 7 T MRI in patients with neuropsychiatric systemic lupus erythematosus. *Neuroreport*. 2015;26(1):27–32. [PubMed: 25426827]
22. Oh BH, Moon HC, Baek HM, et al. Comparison of 7T and 3T MRI in patients with moyamoya disease. *Magn Reson Imaging*. 2017;37:134–138. [PubMed: 27899331]
23. Matsushige T, Kraemer M, Sato T, et al. Visualization and Classification of Deeply Seated Collateral Networks in Moyamoya Angiopathy with 7T MRI. *AJNR American journal of neuroradiology*. 2018;39(7):1248–1254. [PubMed: 29880473]
24. Matsushige T, Kraemer M, Schlamann M, et al. Ventricular Microaneurysms in Moyamoya Angiopathy Visualized with 7T MR Angiography. *AJNR American journal of neuroradiology*. 2016;37(9):1669–1672. [PubMed: 27151748]

25. Seo SW, Kang CK, Kim SH, et al. Measurements of lenticulostriate arteries using 7T MRI: new imaging markers for subcortical vascular dementia. *J Neurol Sci.* 2012;322(1-2):200–205. [PubMed: 22664155]
26. Zwartbol MHT, van der Kolk AG, Kuijf HJ, et al. Intracranial vessel wall lesions on 7T MRI and MRI features of cerebral small vessel disease: The SMART-MR study. *J Cerebr Blood F Met.* 2021;41(6):1219–1228.
27. Shaaban CE, Aizenstein HJ, Jorgensen DR, et al. In Vivo Imaging of Venous Side Cerebral Small-Vessel Disease in Older Adults: An MRI Method at 7T. *AJNR American journal of neuroradiology.* 2017;38(10):1923–1928. [PubMed: 28775055]
28. Berman SE, Clark LR, Rivera-Rivera LA, et al. Intracranial Arterial 4D Flow in Individuals with Mild Cognitive Impairment is Associated with Cognitive Performance and Amyloid Positivity. *Journal of Alzheimer's disease : JAD.* 2017;60(1):243–252. [PubMed: 28826187]
29. Arts T, Meijs TA, Grotenhuis H, et al. Velocity and Pulsatility Measures in the Perforating Arteries of the Basal Ganglia at 3T MRI in Reference to 7T MRI. *Frontiers in neuroscience.* 2021;15:665480. [PubMed: 33981198]
30. Geurts LJ, Zwanenburg JJM, Klijn CJM, Luijten PR, Biessels GJ. Higher Pulsatility in Cerebral Perforating Arteries in Patients With Small Vessel Disease Related Stroke, a 7T MRI Study. *Stroke.* 2018;50(1):Strokeaha118022516.
31. Schnerr RS, Jansen JFA, Uludag K, et al. Pulsatility of Lenticulostriate Arteries Assessed by 7 Tesla Flow MRI-Measurement, Reproducibility, and Applicability to Aging Effect. *Frontiers in physiology.* 2017;8:961. [PubMed: 29225580]
32. Radojewski P, Slotboom J, Joseph A, Wiest R, Mordasini P. Clinical Implementation of 7T MRI for the Identification of Incidental Intracranial Aneurysms versus Anatomic Variants. *AJNR American journal of neuroradiology.* 2021;42(12):2172–2174. [PubMed: 34711553]
33. Samaniego EA, Roa JA, Zhang H, et al. Increased contrast enhancement of the parent vessel of unruptured intracranial aneurysms in 7T MR imaging. *Journal of neurointerventional surgery.* 2020;12(10):1018–1022. [PubMed: 32424006]
34. Gottwald LM, Töger J, Markenroth Bloch K, et al. High Spatiotemporal Resolution 4D Flow MRI of Intracranial Aneurysms at 7T in 10 Minutes. *AJNR American journal of neuroradiology.* 2020;41(7):1201–1208. [PubMed: 32586964]
35. Wrede KH, Dammann P, Johst S, et al. Non-Enhanced MR Imaging of Cerebral Arteriovenous Malformations at 7 Tesla. *Eur Radiol.* 2016;26(3):829–839. [PubMed: 26080795]
36. Wrede KH, Johst S, Dammann P, et al. Improved cerebral time-of-flight magnetic resonance angiography at 7 Tesla--feasibility study and preliminary results using optimized venous saturation pulses. *PLoS One.* 2014;9(9):e106697. [PubMed: 25232868]
37. Cong F, Zhuo Y, Yu S, et al. Noncontrast-enhanced time-resolved 4D dynamic intracranial MR angiography at 7T: A feasibility study. *J Magn Reson Imaging.* 2018;48(1):111–120. [PubMed: 29232026]
38. Dammann P, Wrede K, Zhu Y, et al. Correlation of the venous angioarchitecture of multiple cerebral cavernous malformations with familial or sporadic disease: a susceptibility-weighted imaging study with 7-Tesla MRI. *Journal of neurosurgery.* 2017;126(2):570–577. [PubMed: 27153162]
39. Schlamann M, Maderwald S, Becker W, et al. Cerebral cavernous hemangiomas at 7 Tesla: initial experience. *Academic radiology.* 2010;17(1):3–6. [PubMed: 19910215]

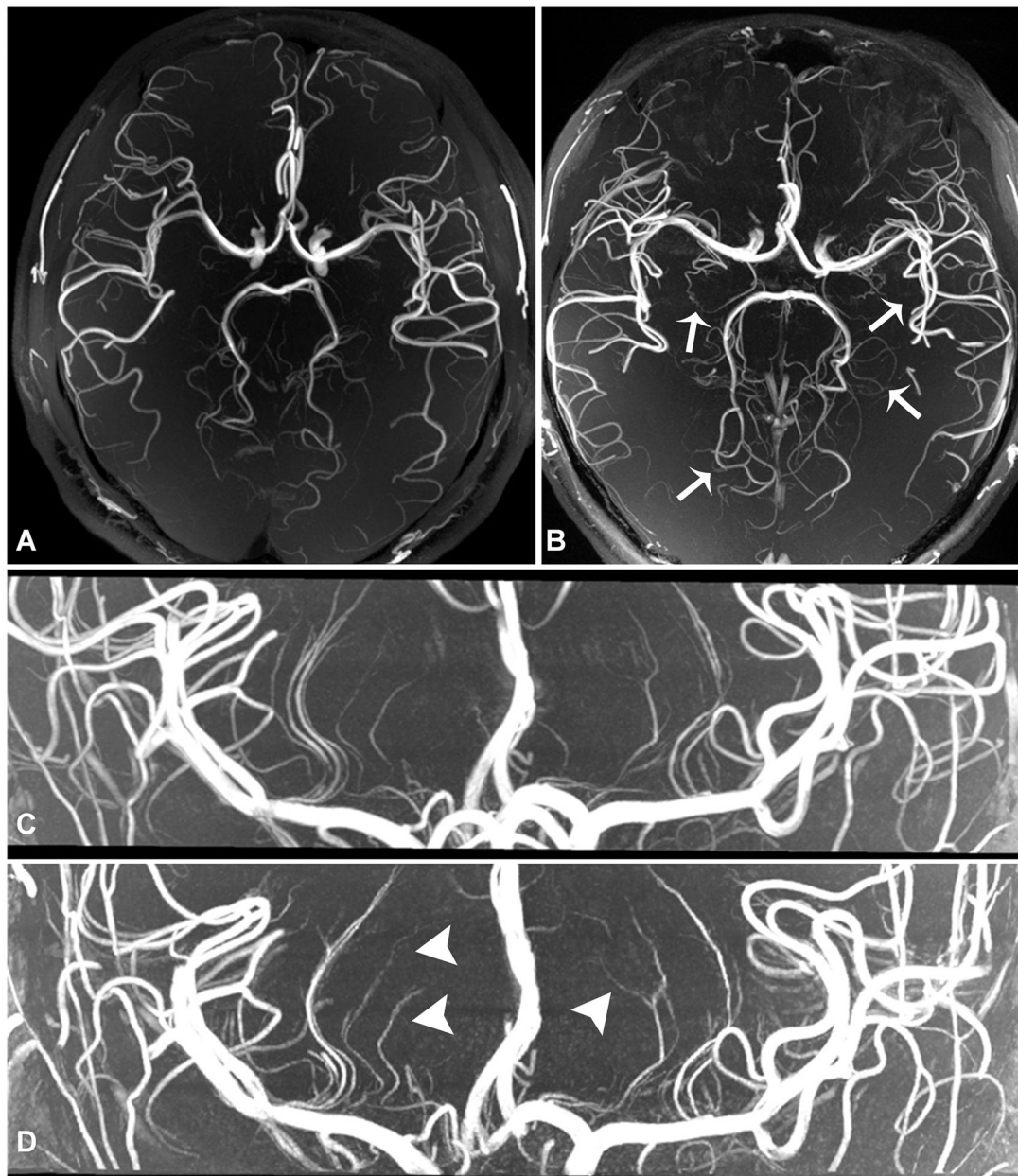


**Figure 1.**

Normal volunteer scan comparison. 3-Tesla 3D TOF-MRA with 0.44 mm isotropic voxel size, acquisition time of 10 minutes 21 seconds (a), shows fewer lenticulostriate and perforator branches than what is seen on 7-Tesla 3D TOF-MRA with 0.3 mm isotropic resolution, acquisition time of 7 minutes 14 seconds (b, arrows). 7-Tesla 3D TOF-MRA with 0.3 mm isotropic resolution (c) compared to 7T TOF-MRA with 0.2 mm resolution, acquisition time 10 minutes 14 seconds (d). There are an increased number of visualized lenticulostriate branches (arrows) at higher resolution acquisition (d, arrowheads), though with use of compressed sensing there is increased noise artifact due to reduced signal, resulting in small branch irregularity.



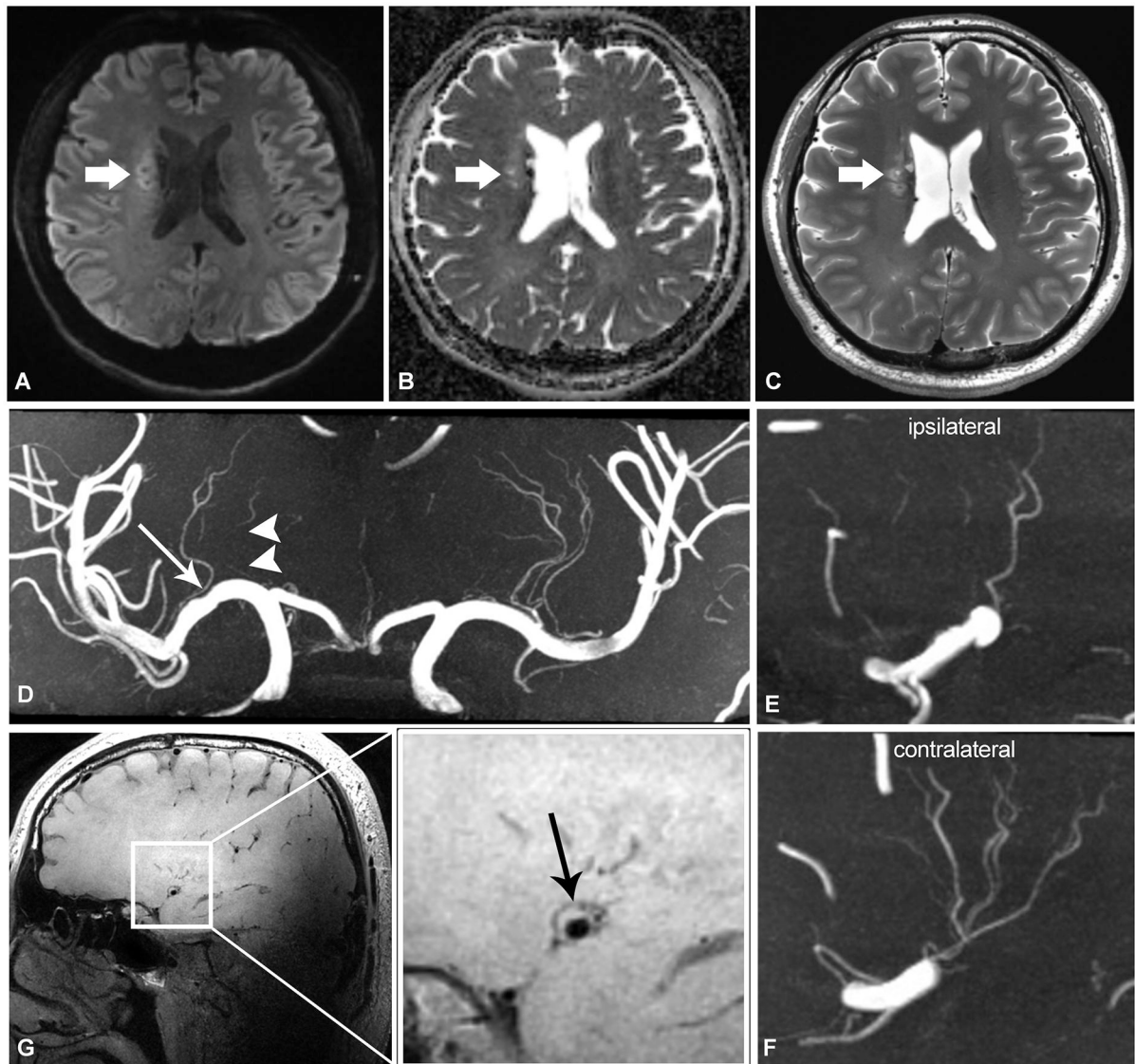


**Figure 2.** Adult patient in their late 30's presenting with left-sided weakness. Axial DWI (a), ADC (b), and T2-weighted (c) sequences show subacute infarct involving the right corona radiata (thick arrows). On TOF-MRA coronal MIP reformat (d), there is mild atherosclerotic irregularity of the right M1 MCA (long arrow), and downstream irregular, discontinuous lenticulostriate branches (arrowheads). There are less lenticulostriate branches originating from the right MCA (e) compared to the left (f). Sagittal T1-weighted VWI (g, and zoomed view) shows plaque along the superior wall of the right MCA (black arrow), at expected location of lenticulostriate branch origins.

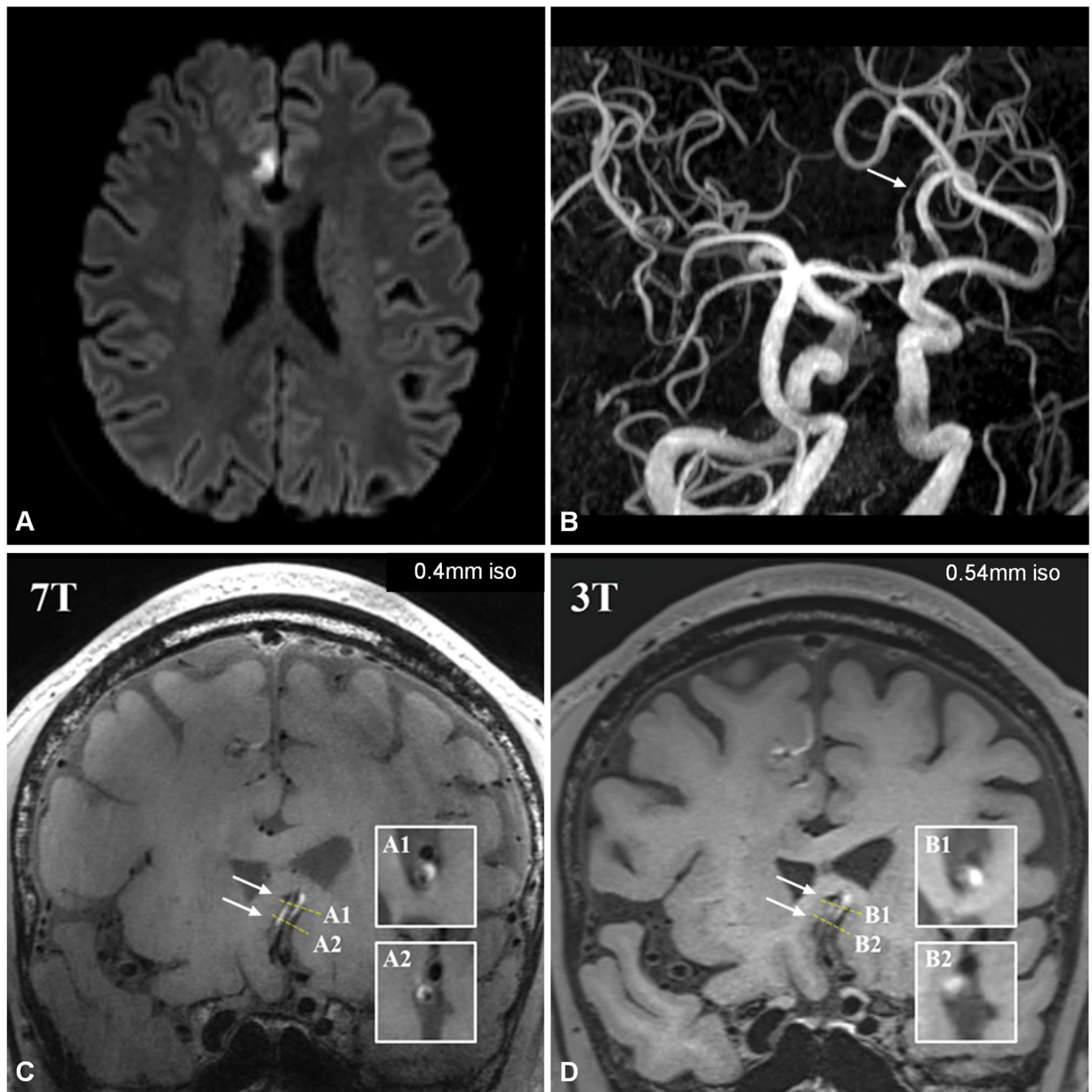


**Figure 3.**

Patient in their early 60's presenting with suspected stroke. Axial DWI (a) shows right medial frontal lobe infarct in right ACA territory. TOF-MRA 3D MIP reconstruction in oblique plane (b) shows stenosis of the A2 ACA bilaterally (arrow). 7-Tesla coronal T1-weighted VWI (c) shows wall hyperintensity involving both ACA's (arrows, A1=cross-sectional slice of left ACA, A2=cross-sectional slice of right ACA), with wall involvement and relationship to lumen being much more conspicuous than on 3T VWI (d). On 3T VWI, it is unclear whether hyperintensity resides within the wall, lumen, or adjacent structures (B1= cross-sectional slice of left ACA, B2=cross-sectional slice of right ACA).



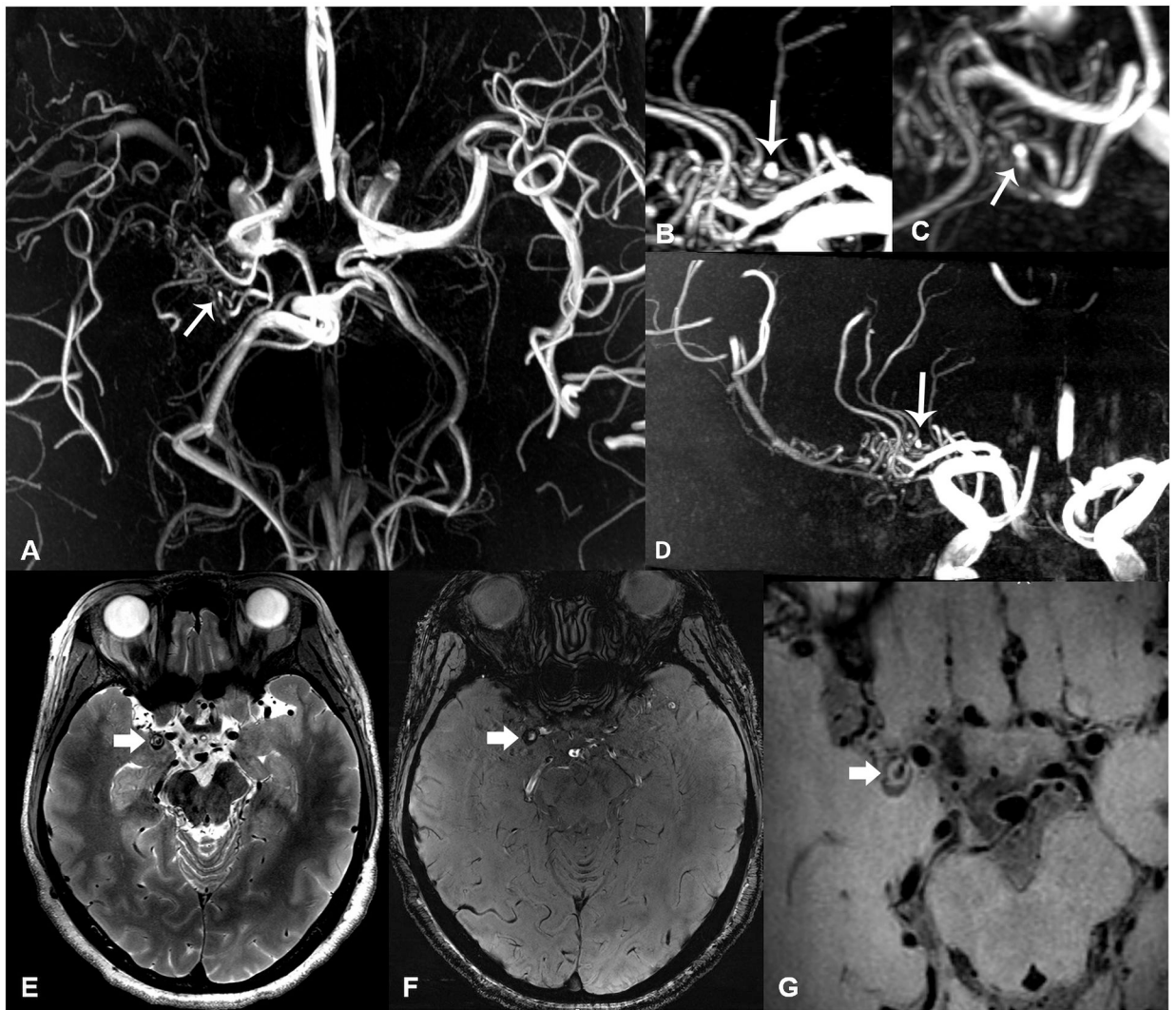


**Figure 4.** Patient in their mid-40's with Moyamoya disease presenting with dizziness for 3 months. 7-Tesla axial (a), sagittal (b), oblique (c) and coronal (d) TOF-MRA MIP reconstructions show right carotid terminus occlusion with extensive pial collaterals, and focal outpouching from collaterals representing micro-aneurysm (arrows). Axial T2-weighted (e), SWI-magnitude (f) and zoomed-in T1-weighted VWI (g) images show an additional small round lesion with heterogenous signal near the right medial temporal lobe, representing a partially thrombosed aneurysm.